CHINESE OPTICS LETTERS

Vol. 22, No. 1 | January 2024

4.096 Tbit/s multidimensional multiplexing signals transmission over 1000 km few mode fiber

Yu Zhang (张 宇)[1], Chen Wang (王 晨)[1], Kaihui Wang (王凯辉)[1], Junjie Ding (丁俊杰)[1], Bowen Zhu (朱博文)[1], Lei Shen (沈 磊)[2], Lei Zhang (张 磊)[2], Ruichun Wang (王瑞春)[2], Changkun Yan (闫长鹃)[2], Bo Liu (刘 博)[3], and Jianjun Yu (余建军)[1*]

[1] School of Information Science and Technology, Fudan University, Shanghai 200433, China

[2] Changfei Optical Fiber and Cable Joint Stock Limited Company, Wuhan 430073, China

[3] Nanjing University of Information Science & Technology, Nanjing 210000, China

*Corresponding author: jianjun@fudan.edu.cn

Received March 14, 2023 | Accepted July 27, 2023 | Posted Online December 29, 2023

We experimentally transmit eight wavelength-division-multiplexing (WDM) channels, 16 quadratic-amplitude-modulation (QAM) signals at 32-GBaud, over 1000 km few mode fiber (FMF). In this experiment, we use WDM, mode division multiplexing, and polarization multiplexing for signal transmission. Through the multiple-input–multiple-output (MIMO) equalization algorithms, we achieve the total line transmission rate of 4.096 Tbit/s. The results prove that the bit error rates (BERs) for the 16QAM signals after 1000 km FMF transmission are below the soft-decision forward-error-correction (SD-FEC) threshold of 2.4×10^{-2}, and the net rate reaches 3.413 Tbit/s. Our proposed system provides a reference for the future development of high-capacity communication.

Keywords: optical fiber communication; mode division multiplexing; few-mode fiber; multiple-input–multiple-output; high-capacity transmission; long-distance transmission.

DOI: 10.3788/COL202422.010602

1. Introduction

In recent years, with the development of the Internet, the volume of global information has grown exponentially, which poses a huge challenge to the existing communication networks[1]. The current communication system based on single-core single-mode fiber, whose communication capacity is basically approaching the limit of Shannon, can no longer meet the demand for the massive growth of communication services. The mode division multiplexing (MDM) technology, which can further improve the transmission rate by increasing the number of channels, has recently received extensive attention from the optical communications industry[2–5]. MDM technology was first proposed in 1982[6]. It takes each mutually orthogonal mode in the optical fiber as an independent channel, and each channel transmits data simultaneously, which can greatly increase the transmission capacity of the communication system[7]. In the past, limited by the development of traditional optical fiber and digital signal processing (DSP) technologies, the cross talk of signals between different modes was strong, and the long-distance transmission of signals could not be realized. The research on MDM was slow. With the advancement of few-mode fiber (FMF), increasingly mature multimode multiplexing and demultiplexing technology, and advanced DSP technologies, it becomes feasible to use FMF for high-capacity long-distance MDM transmission[8–11].

In these years, a great deal of research on MDM transmission systems has been reported in China and abroad[12,13]. In 2018, Li *et al.* transmitted 8-WDM-channels 2-mode 20-GBaud QPSK over 100 km FMF with a transmission rate of 640 Gbit/s[14]. In the same year, Rademacher *et al.* transmitted 381-WDM-channels 3-mode 24.5-GBaud PDM-64-QAM over 30 km FMF with a transmission rate of 280 Tbit/s[15]. In 2019, Soma *et al.* demonstrated a weakly coupled 10-mode-multiplexed transmission with four 4×4 and two 2×2 multiple-input–multiple-output (MIMO) equalizers using PS-PDM-16QAM signals over 48 km FMF, achieving a record transmission capacity of 402.7 Tbit/s[16]. Zhang *et al.* transmitted 80-WDM-channels 8-OAM-mode 16-GBaud QPSK over 50 km ring-core fiber combined with 4×4 MIMO equalizers, and the transmission rate reached 2.56 Tbit/s[17]. In 2020, Shibahara *et al.* achieved 3060 km three-mode signal transmission in the C-band based on weakly coupled FMF with a transmission rate of 40.2 Tbit/s[18]. Zhang *et al.* transmitted 5-WDM-channels two-mode 28-GBaud 16QAM over 5 km FMF based on the direct detection (DD) technique with a transmission rate of 1.12 Tbit/s[19]. In 2021, Rademacher *et al.* transmitted 382-WDM-SDM-channels

Table 1. Records of MDM Transmission Experiments.

Year	Signals/Modes/Distance (km)	Transmission Rate
2018[14]	QPSK/2/100	640 Gbit/s
2018[15]	PDM-64-QAM/3/30	280 Tbit/s
2019[16]	PS-PDM-16QAM/10/48	402.7 Tbit/s
2019[17]	QPSK/8/50	2.56 Tbit/s
2020[18]	16QAM/3/3060	40.2 Tbit/s
2020[19]	16QAM/2/5	1.12 Tbit/s
2021[20]	64QAM/15/23	1.01 Pbit/s
2021[21]	DP-16QAM/2/100	16 Tbit/s

64QAM over 23 km 15-modes FMF with a total data rate of 1.01 Pbit/s[20]. Shen *et al.* transmitted 40-WDM-channels 2-LP-mode DP-16QAM over 100 km weakly coupled DRC-FMF with a total transmission rate of 16 Tbit/s[21]. Table 1 shows some records of the MDM transmission experiments.

In this paper, we demonstrate and verify the transmission over 1000 km FMF. The system adopts IQ modulation/intradyne detection mode, and we combine time-domain least mean square (TD-LMS) and frequency-domain least mean square (FD-LMS) for channel equalization, which has faster convergence speed and higher decision accuracy[22–28]. Thus, we realize the transmission of 8-WDM-channels two-mode dual-polarization 32-GBaud 16QAM over 1000 km FMF, with a net rate of 3.413 Tbit/s[29].

2. Experimental Setup

The experimental setup and the equalization algorithms block diagram used in our work are shown in Fig. 1.

At the transmitter, we first generate a pseudo-random binary series (PRBS) and map it into 16QAM symbols. Then, the 16QAM symbols are upsampled twice, and the baseband is shaped by a root-raised cosine filter. The roll-off factor is set to 0.01. The resampled signal is loaded into an arbitrary waveform generator (AWG, with a maximal sampling rate of 64 GSa/s), and the data transmission rate is set to 32 GBaud.

Eight external cavity lasers (ECLs) generate light waves as laser sources for eight transmission channels (C30–C37), and the output power of each channel is 13 dBm. The AWG outputs two different IQ signals. In the IQ modulators (3 dB bandwidth of 29 GHz), the two signals modulate the WDM signals of four channels, respectively. Then orthogonal polarization multiplexing signals are obtained through the polarization multiplexers. A 1 × 2 coupler couples the two polarization multiplexing signals into one signal. The signal is amplified by an erbium-doped fiber amplifier (EDFA) and then equally divided into two signals by a 1 × 2 coupler. One signal is transmitted through a 3 m delay line to avoid correlation between signals. The two independent signals obtained are used for mode multiplexing. An acousto-optic modulator (AOM) is used for gating the loop input signal. Next, the signal is input into a loop system.

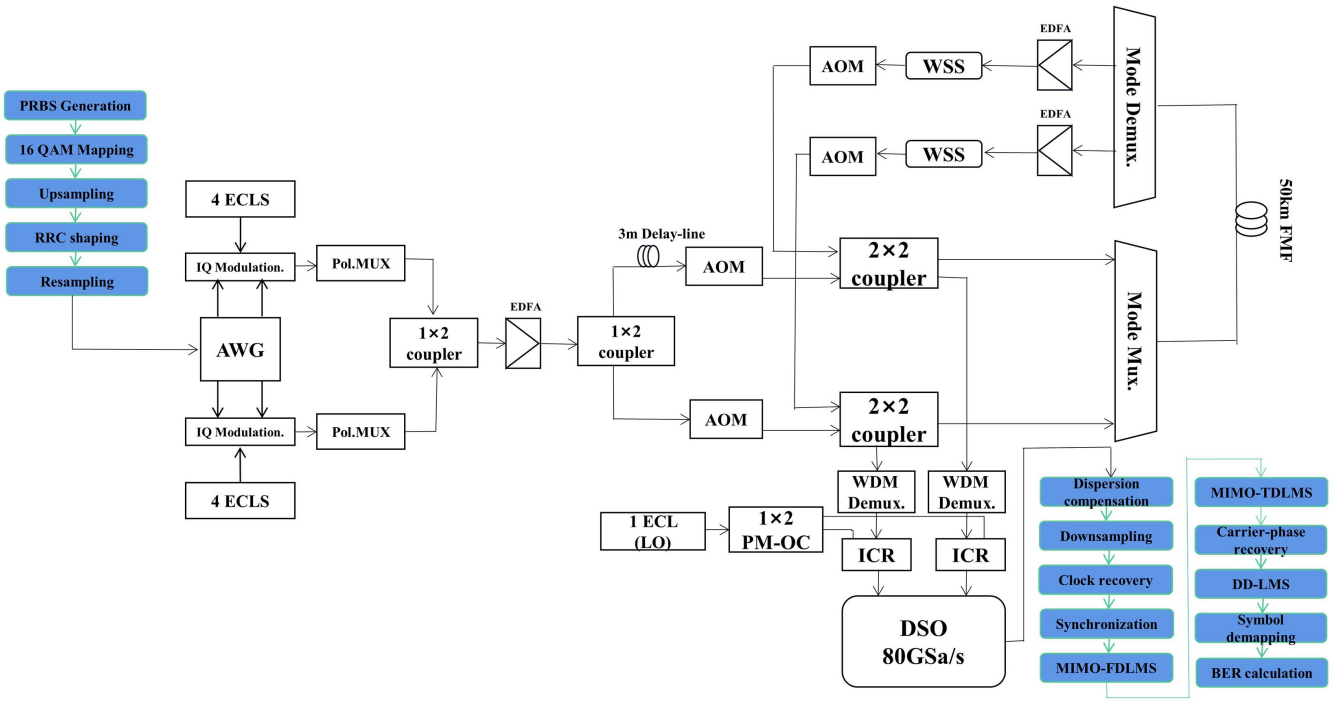

Fig. 1. Experimental setup and equalization algorithms block diagram.

The loop system consists of a six-mode multiplexing pair that is mode-selective (we chose two modes: LP11a and LP11b), a 50 km long FMF, EDFAs, wavelength-selective switches (WSSs, with a maximal insertion loss of 5 dB), and AOMs. Table 2 shows some parameters of the FMF.

After passing through the coupler, the signals are labeled as the LP11a mode and the LP11b mode by the mux mode and fed into the FMF. After being transmitted over the 50 km FMF, the signals are mode-demultiplexed by the demux mode. Due to the correlation loss between modes, which can limit the capacity of the transmission system, each mode is independently compensated with single-mode EDFA for transmission loss. The output power of the two EDFAs in the loop is 16 and 16.6 dBm, respectively. The WSS controls the flatness of each channel of each mode signal after EDFA power balance. After a total of 1000 km transmission through 20 FMF loop systems, the measurement channel signals are selected by WDM demultiplexers, and coherent optical receivers detect the signals. Then the signals are sampled with an oscilloscope at 80 GSa/s with eight synchronized input ports with 33 GHz bandwidth. All sampled signals are processed offline. In order to improve the sensitivity of the receiver and obtain a high signal-to-noise ratio (SNR), we adopt the method of intradyne coherent detection.

In offline DSP, the received signals are firstly compensated for dispersion in the frequency domain, and then downsampled to two samples per signal, followed by clock recovery and synchronization. Moreover, the signals are processed by the MIMO frequency-domain least mean square (MIMO-FDLMS) algorithm, MIMO time-domain least mean square algorithm (MIMO-TDLMS), carrier phase recovery, and direct decision least mean square algorithm (DD-LMS). Finally, the equalized signals are de-mapped by 16QAM and the bit error rate (BER) is calculated. Table 3 shows the parameters of each equalization algorithm.

Table 2. FMF Characteristics.

Parameters of FMF	Numerical Value
Loss (dB/km)	LP01: 0.208 LP11: 0.202
Differential group delay (ps/m)	LP01–LP11: 0.4
Length of single FMF (km)	50
Coefficient of dispersion (ps/(nm × km))	LP01: 21.25 LP11: 21.01
Effective area (μm^2)	LP01: 90 LP11: 121

Table 3. Parameters of Equalization Algorithms.

Equalization Algorithm	Number of Taps	Step Size
MIMO-FDLMS	802	2×10^{-5}
MIMO-TDLMS	401	1×10^{-4}
DD-LMS	401	1×10^{-5}

3. Principles of MIMO-TDLMS and MIMO-FDLMS

Compared to single-channel signal transmission, two-mode dual-polarization transmission signals have greater cross talk after being transmitted through multiple devices and 1000 km FMF, which makes it very difficult to recover each independent signal at the receiver via the DSP. In this experiment, a combination of MIMO-TDLMS and MIMO-FDLMS is used for channel equalization, and the original signals are successfully recovered by the innovative equalization algorithm and other DSPs. MIMO-TDLMS has a slow convergence speed, but a high decision accuracy. MIMO-FDLMS has a low decision accuracy, but a very fast convergence speed. In this paper, the two algorithms are combined to achieve fast convergence speed and high decision accuracy.

In the MIMO-TDLMS algorithm, we use a weight matrix of 16 weight vectors combined in 4 inputs × 4 outputs for signal de-cross talk. Initially, the center position of the weight vector corresponding to the input and output of each weight matrix is set to 1, and the other positions are set to 0. The four-value output from the weight matrix is compared with the training sequence for decision, the error is returned according to the least mean square (LMS) criterion, and the weight matrix W is updated to continue the training. After the error has converged, it changes to the adaptive equalization mode of direct decision, and finally outputs the result. The MIMO-TDLMS algorithm structure and process are shown in Fig. 2.

In MIMO-FDLMS, each signal is upsampled twice and divided into odd and even signals for the fast Fourier transform (FFT). The transformed frequency-domain signal is output and summed through the weight matrix, which is then used as a frequency-domain tapping factor to update and equalize the frequency-domain signal. Unlike the TDLMS, the FDLMS has output and input windows of the same length and runs

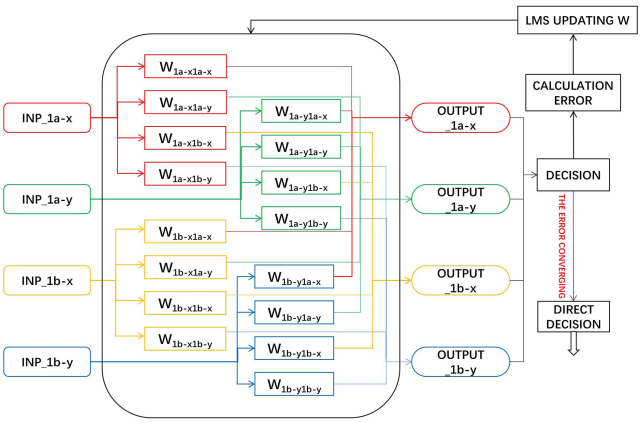

Fig. 2. 4 × 4 MIMO-TDLMS algorithm diagram.

faster, which greatly improves the convergence speed. However, it is necessary to select the appropriate window sliding step to ensure convergence and avoid mutual coupling of signals. Considering the fastest running speed, the window sliding step length can be equal to the window length. It should be noted that at the fastest running speed, the higher the order of MIMO, the greater the computational complexity of the frequency-domain method compared with the time-domain method. After passing the weight matrix, the output sequence is then subjected to the inverse fast Fourier transform (IFFT) to obtain the estimated signal in the time domain. Then the signal is compared, and the error is calculated by the LMS. The return error obtained is again transformed back into the frequency domain by the FFT, and the weight matrix W is updated. After the error has converged, the final result is directly decided and output. The MIMO-FDLMS algorithm structure and process are shown in Fig. 3.

We use the required number of complex multiplication times per symbol output as a measure for algorithm complexity analysis. Assuming that the base 2 FFT algorithm is used in the proposed MIMO-TD/FDLMS algorithm, $(M/2) \times \log_2(M)$ complex multiplication is required each time an FFT operation of length M is performed. Similarly, multiplication of complex vectors in dimension $1 \times M$ once also requires M complex multiplication. Assuming an $n \times n$ MIMO transmission system, the length of the input data in the time-frequency domain is $2M_T$ and $2M_F$, respectively. The forward path of MIMO-FDLMS requires $2n$ times FFT as the time-frequency conversion of input data, the vector multiplication of $2n^2$ dimension M_F is used for frequency-domain equalization, and n times IFFT is used to obtain the time-domain symbol output. The feedback path also requires n times FFT as time-frequency transformation of output data to compute errors and multiply vectors with $2n^2$ dimension M_F for updating filtering coefficients in the frequency domain.

The computational complexity of MIMO-FDLMS is shown in Eq. (1),

$$C_{\text{MIMO-FDLMS}} = ((M_F/2) \times \log_2(M_F) \times 4n + 2 \times M_F \times 2n^2)/(M_F/2). \tag{1}$$

Similarly, the computational complexity of MIMO-TDLMS is shown in Eq. (2),

$$C_{\text{MIMO-TDLMS}} = 2 \times 2M_T \times n^2. \tag{2}$$

As can be seen from the above two formulas, the proposed time-frequency domain combined MIMO-LMS algorithm has the dual advantages of a fast rate of convergence in frequency-domain equalization, as well as low computational complexity and small steady-state error in time-domain equalization, which can obtain the demultiplexed transmission data quickly and effectively.

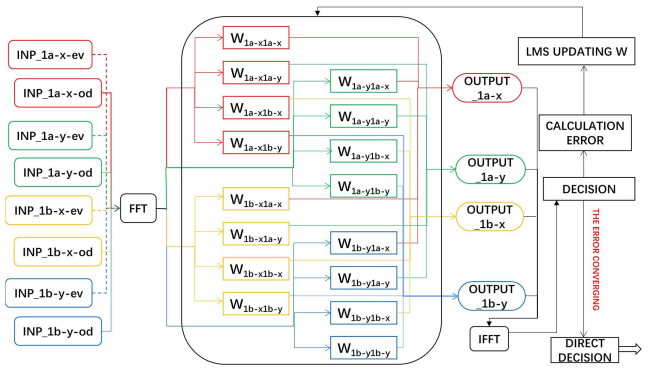

Fig. 3. 8 × 8 MIMO-FDLMS algorithm diagram.

4. Results and Discussion

Figures 4(a) and 4(b) show the optical spectrum before and after transmission over 1000 km. We can find that the optical signal-to-noise ratio (OSNR) difference of each channel is within the range of 2 dB after 1000 km FMF transmission. This indicates that there is some loss in the long-distance transmission of the signal, but it is still recoverable.

We test the BER of the two-mode dual signals in the transmission distance of back-to-back (BTB), 250, 500, 750, and

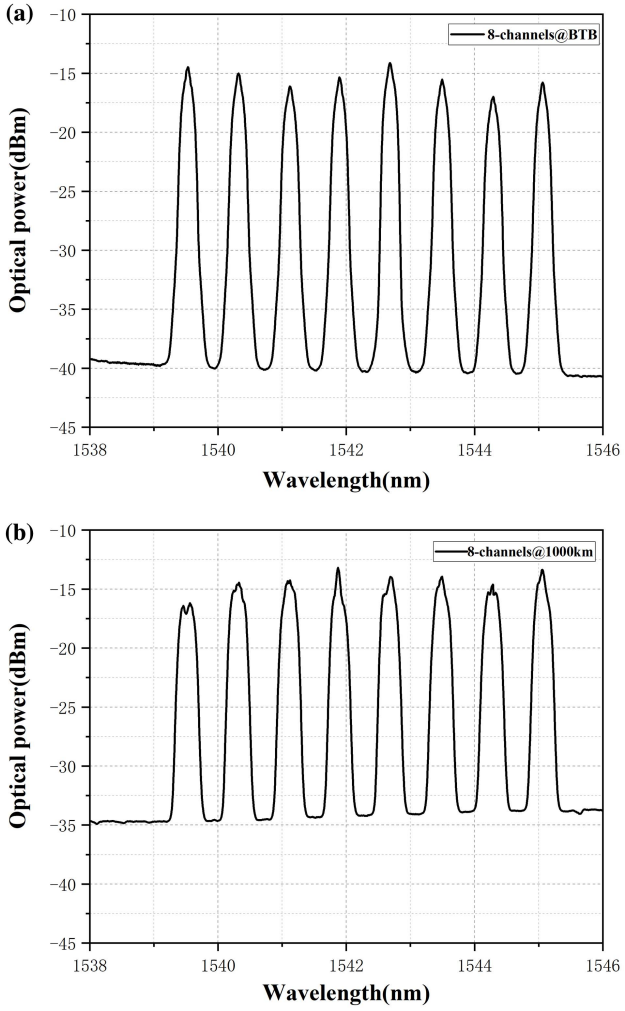

Fig. 4. Optical spectra of (a) BTB and (b) 1000 km.

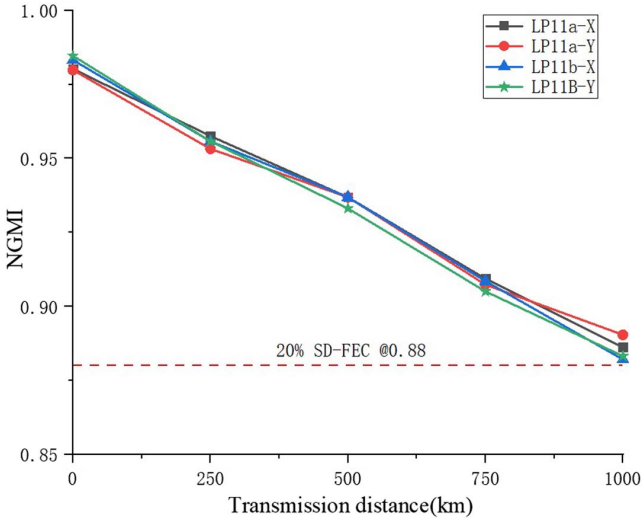

Fig. 5. Transmission performance of different signals at different distances.

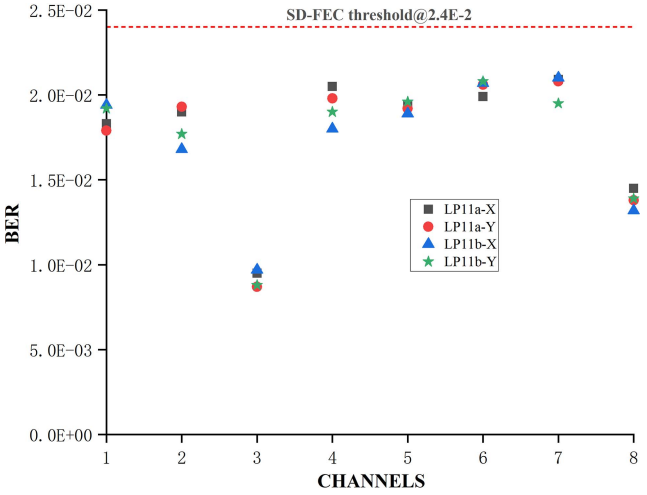

Fig. 7. Performance of C30–C37 eight channels at 1000 km transmission distance.

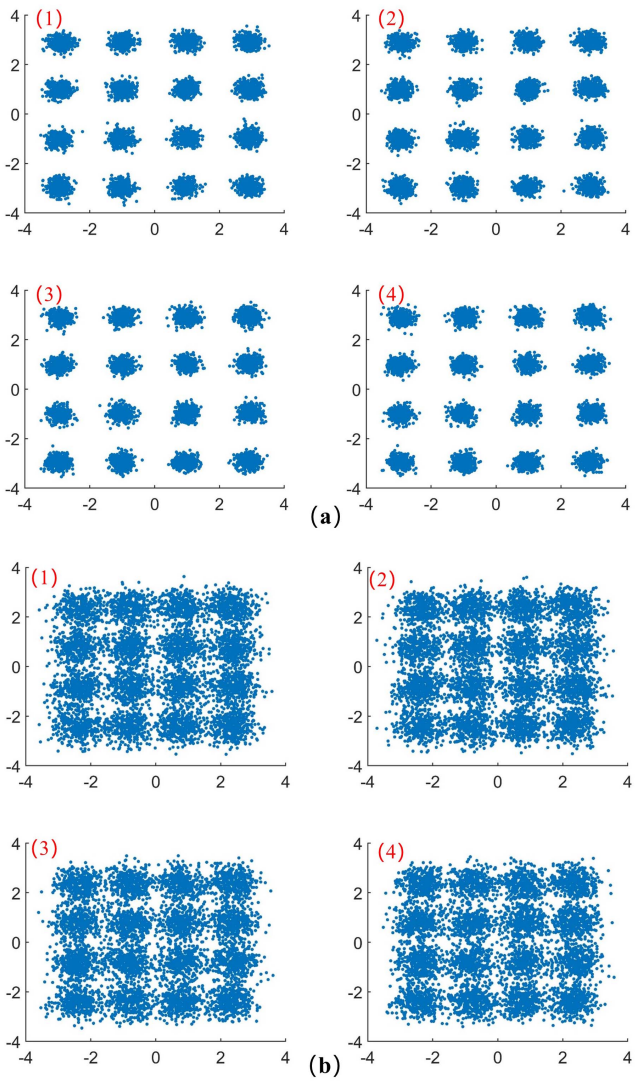

Fig. 6. Constellation diagrams of signals of (a) BTB and (b) 1000 km.

1000 km. Figure 5 shows the generalized mutual information (GMI) of LP11a-Pol.X, LP11a-Pol.Y, LP11b-Pol.X, and LP11b-Pol.Y signals at different transmission distances. Figures 6(a) and 6(b) depict the constellation diagrams of the equalized signals after BTB and 1000 km transmission, respectively. The result shows that the transmission performance of each polarization signal in each mode is basically the same because the two modes of LP11 are degenerate, and the effective refractive index in the multimode fiber is very close, so the BER curve is very close. The BERs of the signals under BTB are all below 10^{-4}. With the increase of transmission distance, the BERs increase gradually. The BER of the four signals is 1.83×10^{-2}, 1.79×10^{-2}, 1.94×10^{-2}, and 1.92×10^{-2}, respectively, at 1000 km transmission, which are all below the SD-FEC threshold of 2.4×10^{-2}.

Figure 7 shows the performance of the eight channels in WDM for the two-mode dual signals at 1000 km transmission distance. Because the wavelength-selective switch (WSS) can control the channel flatness well after EDFA, the BERs of the signals after 1000 km transmission are very close at different EDFA output optical powers, and they are all lower than the SD-FEC threshold of 2.4×10^{-2}. Considering 20% overhead coding, the total net transmission rate is 3.413 Tbit/s (32 GBaud × (4 bit/symbol) × 2 polarizations × 2 modes × 8 channels/(1 + 20%) = 3.413 Tbit/s).

5. Conclusions

In this work, we have built a transmission system based on FMF and successfully achieved the transmission of 32-GBaud 16QAM signals over 1000 km with eight WDM channels in two modes. Two degenerate modes, LP11a and LP11b, and C30–C37 8-WDM channels are selected for transmission over 1000 km FMF with intradyne coherent detection. At the receiver, we innovatively adopt the equalization algorithm combining MIMO-FDLMS and MIMO-TDLMS to remove cross talk,

and the BER of each signal is lower than the threshold of SD-FEC of 2.4×10^{-2}. Finally, we achieve a total transmission rate of 3.413 Tbit/s. The experimental system designed in this Letter provides a feasible scheme for the future development of MDM and long-distance and large-capacity communication transmission. The transmission system is expected to achieve 1–2 orders of magnitude of transmission rate improvement after being combined with multimode multicore fibers[30–32].

Acknowledgements

This work was supported by the National Key R&D Program of China (No. 2018YFB1800905) and the National Natural Science Foundation of China (Nos. 61935005, 61720106015, 61835002, and 62127802).

References

1. J. Yu and Y. Wu, "High-speed optical fiber communication in China," ACS Photonics **10**, 2128 (2023).
2. D. J. Richardson, J. M. Fini, and L. E. Nelson, "Space-division multiplexing in optical fibres," Nat. Photonics **7**, 354 (2013).
3. K. Kitayama and N.-P. Diamantopoulos, "Few-mode optical fibers: original motivation and recent progress," IEEE Commun. Mag. **55**, 163 (2017).
4. P. J. Winzer, "Making spatial multiplexing a reality," Nat. Photonics **8**, 345 (2014).
5. G. Li, N. Bai, and N. Zhao, *et al.*, "Space-division multiplexing: the next frontier in optical communication," Adv. Opt. Photonics **6**, 413 (2014).
6. S. Berdagué and P. Facq, "Mode division multiplexing in optical fibers," Appl. Opt. **21**, 1950 (1982).
7. J. Du, W. Shen, and J. Liu, *et al.*, "Mode division multiplexing: from photonic integration to optical fiber transmission [Invited]," Chin. Opt. Lett. **19**, 091301 (2021).
8. R. Wang, "Research of development status and the trend of optical fiber communication technology," in *4th International Conference on Electrical & Electronics Engineering and Computer Science (ICEEECS)* (2016), p. 1213.
9. J. Xiao, C. Tang, and X. Li, *et al.*, "Polarization multiplexing QPSK signal transmission in optical wireless-over fiber integration system at W-band," Chin. Opt. Lett. **12**, 050603 (2014).
10. F. Yaman, N. Bai, and B. Zhu, *et al.*, "Long distance transmission in few-mode fibers," Opt. Express **18**, 13250 (2010).
11. H. Liu, H. Wen, and G. Li, "Applications of weakly-coupled few-mode fibers [Invited]," Chin. Opt. Lett. **18**, 040601 (2020).
12. S. Beppu, D. Soma, and S. Sumita, *et al.*, "402.7-Tb/s MDM-WDM transmission over weakly coupled 10-mode fiber using rate-adaptive PS-16QAM signals," J. Lightwave Technol. **38**, 2835 (2020).
13. C. Shirpurkar, E. Lucas, and K. Yang, *et al.*, "80-channel WDM-MDM communication link utilizing a photonic crystal resonator and inverse-designed mode-division multiplexers," in *Conference on Lasers and Electro-Optics, Technical Digest Series* (2022), paper STh4N.2.
14. J. Li, C. Cai, and J. Du, *et al.*, "Ultra-low-noise mode-division multiplexed WDM transmission over 100-km FMF based on a second-order few-mode Raman amplifier," J. Lightwave Technol. **36**, 3254 (2018).
15. G. Rademacher, R. S. Luís, and B. J. Puttnam, *et al.*, "93.34 Tbit/s/mode (280 Tbit/s) transmission in a 3-mode graded-index few-mode fiber," in *Optical Fiber Communication Conference* (2018), paper W4C.3.
16. D. Soma, S. Beppu, and S. Sumita, *et al.*, "402.7-Tb/s weakly-coupled 10-mode multiplexed transmission using rate-adaptive PS PDM-16QAM WDM signals," in *45th European Conference on Optical Communication* (2019), p. 1.
17. J. Zhang, Y. Wen, and H. Tan, *et al.*, "80-Channel WDM-MDM transmission over 50-km ring-core fiber using a compact OAM DEMUX and modular 4 × 4 MIMO equalization," in *Optical Fiber Communication Conference (OFC)* (2019), paper W3F.3.
18. K. Shibahara, T. Mizuno, and H. Kawakami, *et al.*, "Full C-band 3060-km DMD-unmanaged 3-mode transmission with 40.2-Tb/s capacity using cyclic mode permutation," J. Lightwave Technol. **38**, 514 (2020).
19. J. Zhang, X. Wu, and L. Lu, *et al.*, "1.12 Tbit/s fiber vector eigenmode multiplexing transmission over 5-km FMF with Kramers-Kronig receiver," in *Optical Fiber Communication Conference (OFC)* (2020), paper W1D.5.
20. G. Rademacher, B. J. Puttnam, and R. S. Luis, *et al.*, "Ultra-wide band transmission in few-mode fibers," in *European Conference on Optical Communication (ECOC)* (2021), p. 1.
21. L. Shen, D. Ge, and S. Shen, *et al.*, "16-Tb/s real-time demonstration of 100-km MDM transmission using commercial 200G OTN system," in *Optical Fiber Communication Conference* (2021), p. 1.
22. J. Yu and X. Zhou, "Novel schemes to generate multi-level modulation formats for ultra-capacity coherent detection transmission systems [Invited Paper]," Chin. Opt. Lett. **8**, 823 (2010).
23. C. Xie, "Nonlinear polarization effects and mitigation in polarization-division-multiplexed coherent transmission systems [Invited Paper]," Chin. Opt. Lett. **8**, 844 (2010).
24. X. Zhou, "Digital signal processing for coherent multi-level modulation formats [Invited Paper]," Chin. Opt. Lett. **8**, 863 (2010).
25. J.-X. Cai, Y. Cai, and C. R. Davidson, *et al.*, "100-Gb/s undersea transmission with high spectral eff iciency using pre-filtered QPSK modulation format [Invited Paper]," Chin. Opt. Lett. **8**, 831 (2010).
26. Y. Jianjun, X. Li, and J. Zhang, *Digital Signal Processing for High-speed Optical Communication* (World Scientific, 2017).
27. J. Yu and N. Chi, *Principles and Applications of Digital Signal Processing Algorithms in High-Speed Optical Fiber Communications (Volume Two): Multi-Carrier Modulation and Artificial Intelligence*, Digital Signal Processing in High-Speed Optical Fiber Communication Principle and Application (Tsinghua University Press, 2018).
28. J. Yu and N. Chi, *Digital Signal Processing in High-Speed Optical Fiber Communication Principle and Application* (Springer, 2020).
29. W.-R. Peng, T. Tsuritani, and I. Morita, "Transmission of high-baud PDM-64QAM signals," J. Lightwave Technol. **31**, 2146 (2013).
30. P. J. Winzer and G. J. Foschini, "MIMO capacities and outage probabilities in spatially multiplexed optical transport systems," Opt. Express **19**, 16680 (2011).
31. T. Hayashi and T. Nakanishi, "Multi-core optical fibers for the next-generation communications," SEI Tech. Rev. **86**, 23 (2018).
32. T. Nakanishi, T. Hayashi, and O. Shimakawa, *et al.*, "Spatial spectral efficiency enhanced multi core fiber," in *Optical Fiber Communication Conference* (2015), paper Th3C.3.